10. G. N. Dul'nev, Yu. P. Zarichnyak, and M. A. Eremeev, "Heat conduction of bound materials," Inzh.-Fiz. Zh., 27, No. 1 (1974).

THEORETICAL AND EXPERIMENTAL INVESTIGATION OF HIGH-LEVEL RADIATION SOURCES USED TO MODEL A HEAT INPUT

V. M. Gradov, B. B. Petrikevich, and A. A. Shcherbakov

UDC 620.172.251.282

This paper examines high-intensity xenon-filled radiation sources for heat load simulation. A mathematical model of the discharge is proposed, and results of a theoretical and an experimental investigation are presented.

One of the main problems which one has to resolve in various branches of technology is that of testing objects under conditions as close as possible to the actual conditions. Many literature references (a detailed bibliography is given in [1]) discuss problems associated with creating facilities to simulate conditions of operation of items of contemporary technology. In some cases a key element of such simulation systems is a high-intensity radiative source (HIRS). A promising HIRS is the pulsed xenon source which has high efficiency in converting electrical into radiative energy, is economical, has a large radiative flux density and high operating stability. To construct a high-efficiency HIRS and to predict its properties reliably requires theoretical and experimental investigations.

The present paper gives some results of mathematical modeling of the working process in a HIRS, determines the limiting characteristics, and describes an experimental investigation. It should be noted that in natural-model thermal endurance tests an HIRS may operate in a heater system comprising several sources and reflectors. The investigation and the development of an HIRS incorporated into a facility requires the development of a complete system for computer design of such facilities, based on methods of designing and testing of an individual isolated HIRS.

Mathematical Model of the Discharge. We assume that the plasma is in a state of local thermodynamic equilibrium (LTE). The system of energy balance and radiative transfer equations describing the physical processes in the discharge takes the form

$$\frac{1}{R^2 z}\frac{d}{dz}\left[z\lambda_r(T)\frac{dT}{dz}\right]+\sigma(T)E_1^2-\operatorname{div}F_r=0, \tag{1}$$

$$\frac{1}{3R^2 z}\frac{d}{dz}\left[z\frac{1}{K'_{\nu\Sigma}}\frac{du_\nu}{dz}\right]+K'_{\nu\Sigma}(u_{\nu e}-u_\nu)=0, \tag{2}$$

$$\operatorname{div}F_r=c\int_0^\infty K'_{\nu\Sigma}(u_{\nu e}-u_\nu)\,d\nu. \tag{3}$$

The boundary conditions are

$$z=0,\quad \frac{dT}{dz}=0,\quad \frac{du_\nu}{dz}=0, \tag{4}$$

$$z=1,\quad T=T_w,\quad u_\nu=-\frac{A}{RK'_{\nu\Sigma}}\frac{du_\nu}{dz}. \tag{5}$$

Here we neglect convection and postulate that the voltage E_1 is constant along the arc. Equations (2) and (3) describe radiative transfer in the diffusion approximation. According to the data of [2], the constant A = 0.847.

N. É. Bauman MVTU. Translated from Inzhenerno-Fizicheskii Zhurnal, Vol. 38, No. 3, pp. 450-456, March, 1980. Original article submitted November 15, 1977.

 0022-0841/80/3803-0262$07.50

The agreement of results of calculations using the mathematical model adopted depends strongly on the accuracy of the material functions σ, λ_T, and especially $K'_{\nu\Sigma}$, since the main form of energy transfer in high-power discharges is radiative transfer; σ and λ_T for a xenon plasma have been calculated and measured by a number of authors, to sufficient accuracy for practical purposes. Here we use the results of [3, 4].

The value of $K'_{\nu\Sigma}$ was calculated [5], accounting for the following radiative processes: photoionization of the atoms and first ions of Xe, brehmsstrahlung processes in the atoms and ions of Xe, and the XeI lines, broadened by various mechanisms. The bound-free absorption coefficient is determined using photoionization cross sections of [6] by direct summation over levels. Bremsstrahlung processes in the ions are accounted for by means of the ξ-factor [5, 7], and here we used the fact that the quantum defects of the levels are independent of energy. The free–free transitions in the fields of neutral atoms, according to estimates we made, give a negligibly small contribution to $K'_{\nu\Sigma}$ in the region examined: frequency $\nu = 0.02 - 3 \cdot 10^{15}$ Hz, temperature 2000-20,000°K, pressure 5-25 atm. In the discrete spectrum we considered in detail the first terms of the spectral series formed by transitions to the 6s, 6p, 6s', 5d, $5p^6\ {}^1S_0$ levels. Of the various mechanisms for line broadening we took into account the Stark, Doppler, resonance, and Van der Waals.

A numerical solution of the system of equations (1)-(3) was performed by a time-dependent method [8], which was chosen to avoid instabilities appearing when other methods are used (Runge–Kutta, Adams–Krylov). A finite-difference approximation to the equations was written in implicit form, and the system of algebraic equations obtained was solved by a marching method.

By solving the system (1)-(3) we found the temperature profile in the plasma, the potential E_1, the heat flux F_T, and the radiant flux F_r incident on the wall of the discharge tube, the spectral flux $F_{r\nu}$, and the spectral flux $F'_{r\nu}$, which passes through the discharge tube wall, the coolants, and the outer envelope, accounting for the actual transmission curves of these, and the initial Xe pressure at the given operating efficiency η_{HIRS} of the HIRS.

Determination of Limiting Characteristics. In calculating the limiting operating conditions of a continuous HIRS one must take into account that there are two possible causes of breakdown of operation of a gas-discharge tube: the tube wall temperature can exceed some limit T_{lim}, leading to crystallization of the quartz at a certain rate, and the wall material can reach a limiting state of stress, i.e., the tube breaks up under mechanical stresses σ_{lim}. These stresses are due to internal pressure and the nonuniformity of heating.

The equation describing the thermal state of the discharge tube wall has the form

$$\frac{d}{dx}\left[\lambda_w(T_w)\frac{dT_w}{dx}\right] + (F_T + F_r)\int_0^{\nu_l}\eta_\nu K_\nu \exp[-K_\nu x]\,d\nu = 0. \tag{6}$$

The boundary conditions are

$$x = 0, \quad \lambda_w(T_1)\frac{dT_w}{dx} = -F_T^{eff}, \tag{7}$$

$$x = h_1, \ \lambda_w(T_2)\frac{dT_w}{dx} - \alpha(T_2 - T_c) = 0, \tag{8}$$

$$\eta_\nu = F_{r\nu}/(F_T + F_r).$$

Beyond the quartz transmission boundary the radiative energy absorption occurs in a thin surface layer. This is accounted for in boundary condition (7) by introducing the quantity

$$F_T^{eff} = F_T + \int_{\nu_l}^{\infty} F_{r\nu}\,d\nu. \tag{9}$$

The wall of a cylindrical discharge tube is considered as planar. The admissibility of this substitution is discussed in [9]. The solution of Eq. (6) has the form

$$T_w(x) = \left\{\frac{\Theta^n(F_T + F_r)(n+1)}{\lambda_0}\left[-\int_0^{\nu_l}\frac{\eta_\nu}{K_\nu}\exp[-K_\nu x]\,d\nu - x\right] + \right. \tag{10}$$

$$\left. + \left[T_c - \frac{F_T + F_r}{\alpha}\right]\left(\int_0^{\nu_l}\eta_\nu \exp[-K_\nu h_1]\,d\nu - 1\right)^{n+1} + \frac{\Theta^n(F_T + F_r)(n+1)}{\lambda_0}\left(\int_0^{\nu_l}\frac{\eta_\nu}{K_\nu}\exp[-K_\nu h_1]\,d\nu + h_1\right)\right\}^{1/(n+1)}.$$

Hence it is easy to find the temperature T_1 on the inner surface of the tube.

Using the results of [10], we can write expressions for the circumferential σ_Θ, axial σ_0, and radial σ_r stresses in the form

$$\sigma_\Theta(r) = \frac{\alpha_1 E}{1-\nu_1}\frac{1}{r^2}\left(\frac{r^2+R^2}{b^2-R^2}\int_R^b T_w(r)\,rdr + \int_R^r T_w\,rdr - T_w r^2\right) + \frac{pR^2(r^2+b^2)}{r^2(b^2-R^2)}, \tag{11}$$

$$\sigma_0(r) = \frac{\alpha_1 E}{1-\nu_1}\left(\frac{2}{b^2-R^2}\int_R^b T_w(r)\,rdr - T_w r^2\right) + \frac{pR^2}{b^2-R^2}, \tag{12}$$

$$\sigma_r(r) = \frac{\alpha_1 E}{1-\nu_1}\frac{1}{r^2}\left(\frac{r^2-R^2}{b^2-R^2}\int_R^b T_w(r)\,rdr - \int_R^r T_w(r)\,rdr\right) + \frac{pR^2(r^2-b^2)}{r^2(b^2-R^2)}, \tag{13}$$

where R and b are the inner and outer radii of the envelope.

With Eqs. (10)-(13) one can solve the problem of determining the limiting characteristics of an HIRS (from the viewpoint of operability of the envelope). Depending on the limiting parameter (T_{lim} or σ_{lim}), the governing quantity may be the voltage or the temperature. At large pressures the stresses due to internal pressure are high. As the wall thickness increases the thermal stress increases and the stress due to pressure decreases. Therefore, at large pressure ($p \sim 20$ atm) there is an optimal envelope thickness.

Experimental Investigations and Discussion of Results. Of the large set of experimental investigations we can single out three basic types:

1) an experimental check of the computational and theoretical models of the working process in the HIRS;

2) an experimental check of the elements and of the HIRS structure as a whole;

3) a test of material specimens and of structural elements by means of the HIRS facilities that have been developed.

The first group of investigations is based on a check of agreement between the design values and the experimentally determined HIRS output parameters, such as the efficiency, the volt–ampere characteristics, etc.; the second group is done as an experimental check of the suitability of various materials for construction of HIRS components, and also to check the operability of the elements and the HIRS structure as a whole; the aim of the third group is to determine the speed of propagation of temperature waves in the material, to measure the temperature field in the specimen, etc..

To conduct the entire set of experiments we designed and built a facility which included the hydraulic system, the electrical supply system, the control and automation system, the measurement system, and the gas system.

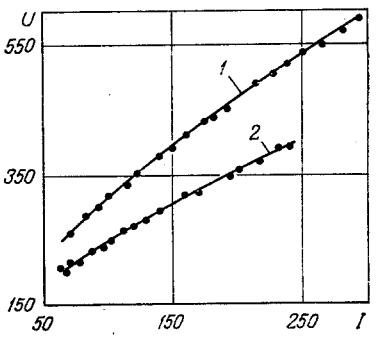

Fig. 1. Volt–ampere characteristics of the HIRS: 1) $R = 0.6 \cdot 10^{-2}$ m; $p_0 = 300$ torr (HIRS-50); 2) $R = 0.35 \cdot 10^{-2}$ m; $p_0 = 300$ torr (HIRS-20); the curves are theory; the points are the experiment. U is in V, and I is in A.

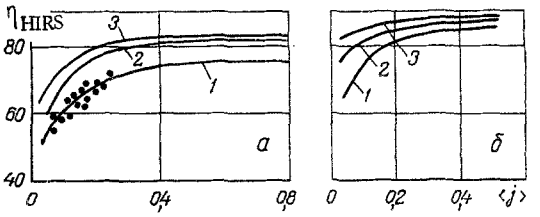

Fig. 2. HIRS efficiency: a) $R = 0.35 \cdot 10^{-2}$ m; b) $R = 0.8 \cdot 10^{-2}$ m; 1) $p = 5 \cdot 10^5$ N/m^2; 2) $15 \cdot 10^5$; 3) $25 \cdot 10^5$; the curves are theory; the points are experiment. η_{HIRS}, %; $\langle j \rangle$, kA/cm^2.

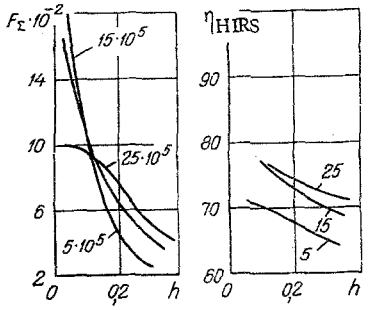

Fig. 3. The limiting total energy flux on the wall and the efficiency of the HIRS as a function of the wall thickness and the plasma pressure. $R = 0.35 \cdot 10^{-2}$ m. The numerals on the curves are the plasma pressure, in N/m^2. $F_\Sigma \cdot 10^{-2}$ is in W/cm^2, h is in cm.

Figure 1 shows the theoretical and experimental volt–ampere characteristics of the HIRS-20, with an interelectrode distance of 200 mm, and of the HIRS-50, with an interelectrode distance of 500 mm. It should be noted that the mathematical model of the discharge takes rather fully into account the processes occurring in a xenon discharge plasma. Figure 2 shows data on the experimental and theoretical efficiency of the HIRS, this being defined as the ratio of the integral radiative flux passing the wall of the discharge tube, the cooler, and the outer envelope, to the electrical power developed in the HIRS. For the calculated efficiency we assumed transmission curves for domestic quartz with a transmission limit of $\nu_b = 1.25 \cdot 10^{15}$ sec^{-1}. From the results presented it can be seen that for the low-power conditions achieved in the type HIRS-20, the efficiency lies in the range 60–70%. To increase the efficiency one must design a HIRS with a higher operating voltage.

Some of the results on limits of the electrical power F_Σ, transferred per unit surface area, and on the HIRS efficiency, are shown in Fig. 3. We assumed values of 1600°K and $3 \cdot 10^7$ N/m^2 for T_{lim} and σ_{lim}, respectively. It can be seen from Fig. 2 that the highest characteristics correspond to the small wall thickness ($h_1 < 0.1$ cm). A reduction of the working pressure in the HIRS increases F_Σ. Since a pressure reduction lowers the HIRS efficiency, the optimal pressure, giving the greatest radiant flux, should evidently be $p = 15 \cdot 10^5$ N/m^2, for the above values of T_{lim} and σ_{lim}. When the tube radius is increased to 0.8 cm, the pressure optimum is displaced to $5 \cdot 10^5$ N/m^2, and here as before a low wall thickness is preferable, and the radiative output increases by a factor of 1.2 to 1.3 compared with the R = 0.35 cm case.

Figure 4 shows experimental data on the rate of specimen surface temperature increase for various materials. The heating was accomplished either with one HIRS-20, or by KI-type infrared lamps, which are currently widely used for heating of large-size material specimens and structures. Analysis of the results obtained shows that their use is preferred as heaters in high-power radiative sources.

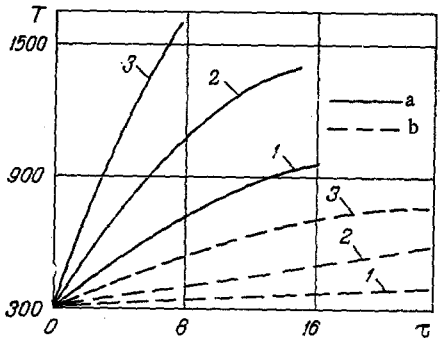

Fig. 4. Experimental determination of the heating rate: a) heating of the HIRS-20; b) heating with KI infrared lamps; 1) type M2 copper; 2) type St.45 steel; 3) type Kh18N9T steel. T, °K; τ, sec.

NOTATION

r, current radius; R, discharge tube radius; $z = r/R$, relative radial coordinate; F_r, integral radiative flux; u_ν, radiant energy density; $u_{\nu e}$, energy density of equilibrium radiation; c, speed of light; T_W, wall temperature; λ_T, thermal conductivity; σ, electrical conductivity; $K'_{\nu\Sigma}$, total plasma absorption coefficient; ν, frequency; $\lambda_W(T_W) = \lambda_0(T_W/\Theta)^n$, thermal conductivity of the wall material (for quartz $\lambda_0 = 0.014$ W/deg·cm, $n = 1/3$; $\Theta = 293°K$); T_1, T_2, temperatures on the inner and outer surfaces of the tube; T_c, cooler temperature; K_ν, spectral absorption coefficient of the wall material; γ_l, limiting frequency for radiative transmission of the wall material; h_1, wall thickness; α, heat removal coefficient; E, elastic modulus for elongation and compression; ν_1, Poisson coefficient; h, Planck constant; $\langle j \rangle$, current density.

LITERATURE CITED

1. G. I. Petrov (editor), Modeling of Thermal Conditions for Spacecraft and Their Environment [in Russian], Mashonostroenie, Moscow (1971).
2. J. J. Lowke and E. R. Capriotti, "Calculation of temperature profiles of high-pressure electric arcs using the diffusion approximation for radiative transfer," JQSRT, 9, 207 (1969).
3. Yu. G. Basov, V. V. Ivanov, V. N. Makarov, G. I. Narkhova, and A. A. Shcherbakov, "Influence of a laser illumination on the characteristics of a pumping source," Opt. Spectrosk., 38, 608 (1976).
4. R. S. Devoto, "Transport coefficients for partially ionized krypton and xenon," Raket. Tekh. Kosmon., No. 2, 10 (1969).
5. V. M. Gradov, A. A. Mak, and A. S. Shcherbakov, "Computation of the optical characteristics of a xenon plasma, allowing for the effect of envelope erosion products," Opt. Spektrosk., 43, 207 (1977).
6. A. Burgess and M. Seaton, "A general formula for the calculation of atomic photoionization cross sections," M. N. R. Astron. Soc., 120, 121 (1961).
7. L. M. Biberman and G. É. Norman, "Continuum spectra of atomic gases and plasma," Usp. Fiz. Nauk, 91, 193 (1967).
8. S. K. Godunov and V. S. Ryaben'skii, Computational Schemes [in Russian], Nauka, Moscow (1973).
9. V. N. Eliseev, "Computation of the temperature of the cooled cylindrical envelope of a plasma discharge," Svetotekhnika, No. 3, 6 (1969).
10. S. P. Timoshenko and J. N. Goodier, Theory of Elasticity, McGraw-Hill (1970).